Characterisation of Human Body Shadowing in Millimetre Wave Systems

*Khalid A. Al Mallak, *Manish Nair, *Geoffrey Hilton, **Tian H. Loh and *Mark A Beach

*Electrical and Electronics Engineering, University of Bristol (UoB), Bristol, UK
** National Physical Laboratory (NPL), Teddington, UK
*k.almallak, qx20364, geoff.hilton, m.a.beach@bristol.ac.uk
**tian.loh@npl.co.uk

***Abstract*—One of the main challenges in millimetre wave (mm-wave) communication for fifth-generation (5G) and beyond systems is the shadowing of received signals. A mobile device in proximity to a human body can result in shadowing of the received mm-wave signal. By investigating different antenna heights, it is possible to model shadowing based on which, the channel capacity and the resulting average attenuation in the shadow region of the human body is derived. It is proven that the attenuation in the body's shadow for a mm-wave signal at 26GHz can be reduced when the transmit and receive antenna heights are adjusted. Forwards and backwards movement of the body causes positive and negative Doppler Shift, respectively, producing frequency dispersion, in addition to the channel delay-dispersion. It is also demonstrated that a steerable beam reduces the signal attenuation in the shadow region significantly, as the delay-dispersion of the channel reduces.**

***Index Terms*—Beamwidth, delay spread, Doppler shift, indoor, mean blockage attenuation, millimetre wave, shadow, static human body, 5G.**

I. Introduction

Millimetre wave (mm-wave) communications is expected to provide high data-rate and low-latency services. There are several challenges observed when the technology is implemented in the fifth-generation (5G) and beyond communication systems. These include maintaining the high directivity between the transmitter and the receiver. A significant challenge is the vulnerability of the mm-wave signals to blockages which causes shadowing, such as from that of a human body, especially in crowded hot spots such as railway stations and busy office environments [1]. When moving or changing the position of a user device, the instantaneous dynamics of the channel change.On many occasions, it is necessary to change the position of the mobile device to get better reception although this could be interpreted as a poor quality mm-Wave device. Furthermore, [2] showed that even the human body mass and the type of clothes have an impact on the quality of the mm-wave signal. This paper[1] reports the measurements conducted recently at the University of Bristol (UoB) Communications and Systems Network (CSN) Lab to investigate the human body shadow on a 26GHz mm-wave signal.

[1]This research was sponsored through the EPSRC CDT in Communications (EP/L016656/1) and NPL.

The key contributions of this paper are based on measuring the mm-wave signal attenuation in the shadow region of the human body for an indoor environment when the receive (Rx) antenna is positioned next to the waist or near the chest of a human using the aforementioned 26GHz mm-wave signal with 1GHz bandwidth. It also presents:

- The investigation includes reference measurements performed in the Anechoic chamber with and without the human body at a safe distance, and in the CSN Lab without human body.
- Different transmit (Tx) and Rx heights are investigated to report the positions where the lowest signal attenuation is realised and how the channel dispersion responses are obtained based on the analysis of the root mean square-delay spread (RMS-DS). The measurements are performed in such away that the Rx antenna is next to a static volunteer during the first 4.5s or the last 4.97s of measurement time, and, before the volunteer moves away or towards Tx antenna, respectively, in order to measure the signal attenuation.
- The shadow regions are modeled to obtain the coefficient of shadowing in Watts/m based on which the channel capacity is derived.

This paper is divided into four sections. Section II covers some of the theory related to the attenuation produced by the human body. It is followed by measurements setup and modelling in Section III. Section IV presents the results with the analysis, which followed by conclusions in Section V.

II. Conceptual Background

To reduce the impact of a human body blockage in the shadow region, either the antenna's position at Rx should re-positioned, or the Tx antenna's beamwidth should adjusted towards the direction of the Rx antenna. Furthermore, by adjusting the beamwidth or using antennas array it will be possible to mitigate the impact of human body shadow [3] [4]. The shadowing effect of a human body was simulated at 28GHz and 60GHz presuming a user is using a mobile phone for browsing with a single or two hands grip [5]. However, no real human body shadowing was investigated and only a static person was considered. Furthermore, the shadowing observed in a busy environment because of the pedestrians has signal attenuation

inversely proportional to Tx/Rx antenna's half-power beamwidth (HPBW), because larger beamwidth can capture more energy diffracted around human in blocking region [6]. Therefore, the mean blockage attenuation (MBA) observed in dense area, can be computed as [6]

$$\text{MBA (dB)} = 10\log\left(b + \frac{180}{\text{HPBW}}\right) \quad (1)$$

where b is a constant which sets to be 9.8 for a busy environment with many obstacles. If a less busy environment is to be studied, then b should have a lower value. For the measurements performed recently in the CSN Lab, a horn antenna with HPBWs between $17^\circ - 25^\circ$ and gains between 13.1dB and 12.3dB correspondingly, are used. In [7] different models are developed when a human body obscures the line-of-sight (LoS) between Tx and Rx antennas.

III. Models & Measurement Setup

A. Development of Shadow Model

A model is developed based on the illustration of shadow and non-shadow regions when the volunteer walks forward and backward as shown in Fig. 1(a) and Fig. 1(b) based on the parameters given in Table I. The waist size of the volunteer is 36cm indicating that the region behind the volunteer is the shadow region. Firstly, the width of the non-shadow region can be obtained from geometry as (see Fig. 1)

$$w = d \cdot \tan(\frac{\text{HPBW}}{2}) \quad \text{m} \quad (2)$$

where d is the distance traversed whilst walking backwards or forwards between Tx and Rx which is 5m and 4m as in Fig. 1(a) and Fig. 1(b) correspondingly. Then, the shadow coefficient χ in Watts/m can be derived as

$$\chi = \frac{1}{2w - 0.36\text{m}}\left(\frac{P_{rx}}{\text{SNR}} - \sigma^2\right) \quad \text{Watts/m} \quad (3)$$

where 0.36m is the waist size of the volunteer. P_{rx} and the signal-to-noise ratio (SNR) are measured and σ^2 is the variance of the additive white Gaussian noise (AWGN). The channel capacity is then derived and computed based on Shannon equation as 4 [8].

$$C = B \cdot \log_2\left(1 + \frac{P_{rx}}{\chi \cdot d + \sigma^2}\right) \quad (4)$$

where $B = 1$GHz is the bandwidth of the mm-wave system. Lastly, It is worth noting that the channel capacity derived based on the Shannon equation

$$C = B \cdot \log_2\left(1 + 10^{\frac{pl}{10}}\right) \quad (5)$$

where pl, the the path-loss obtained from the measurements after conversion to linear scale as $pl = P_t(\text{dBm}) - P_{rx}(\text{dBm})$ is an exact match the channel capacity derived in (4). This validates the model.

B. Measurement Setup

This research fundamentally aims to investigate the mm-wave signal attenuation produced by a human body when a mobile device is in the pocket, i.e., within the shadow region. Two measurements setups depicted in Fig. 2, Fig. 3 and Fig. 4 with setup values shown in Table I are performed within the Anechoic chamber and outside (CSN Lab). The results observed inside

TABLE I: Measurement Setup

Setup	Value
htx	1.5-2 m
hrx	0.93-1.4 m
freq	26 GHz
BW	1 GHz
Tx-Rx distance	4 m
Polarisation	Horizontal
PTx	14 dBm
HPBW	17°

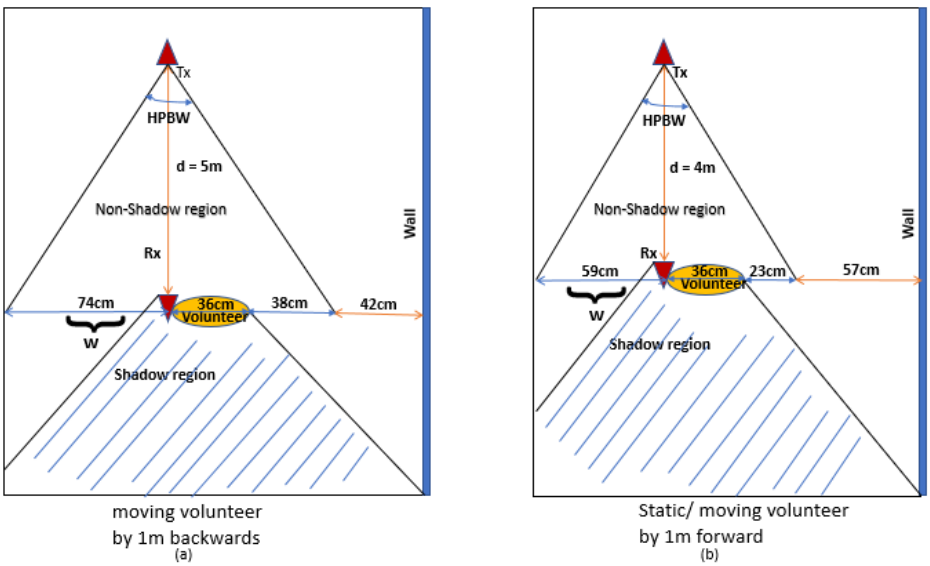

Fig. 1: Shadowing models for (a) for a volunteer walking backward and (b) for a volunteer walking forward.

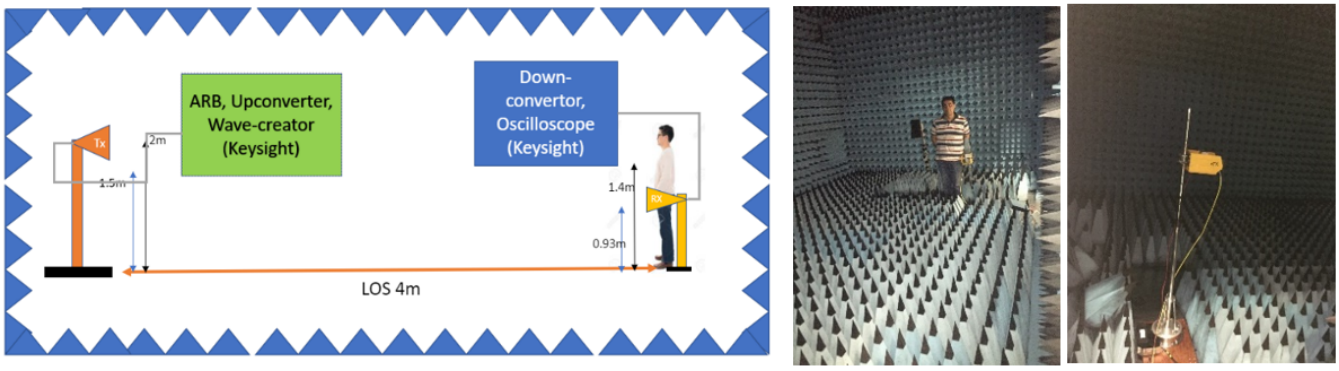

Fig. 2: Reference measurements of the CIR using the UoB channel sounder in Anechoic chamber at a safe distance.

the Anechoic chamber are used as reference measurements to compare them with the measurements done outside in the CSN Lab with a static and moving human body. However, further reference measurements are also then performed in the CSN Lab to validate the results observed with the existence of a human body. The environment is unchanged during the measurement time to keep the results consistent. Furthermore, three runs are performed for each measurement with and without human body at a different Tx and Rx antenna heights h_{tx} and h_{rx} correspondingly. Each run takes about 4.97sec to complete. The UoB channel sounder[2] is used to record P_rx, SNR and RMS-DS [9]. Moreover, the received power is measured, enabling the recording of the channel dispersion time of all multipath components (MPCs).

IV. Results & Analysis

A. Reference Measurements in the Anechoic Chamber on a Static Volunteer

The measurement setup depicted in Fig. 2 is characterised by the received power and attenuation produced when Rx antenna is fixed to the waist of a standing human body during the static measurements. Further, since the attenuation is a measure of the dB difference between the transmit power (P_{tx}) and the receive power (P_{rx}), the mm-wave signal attenuation observed outside the shadow region (of the human body) for antenna heights h_{tx} and h_{rx} are significantly lower as compared to the other h_{tx} and h_{rx} heights.

[2]The Channel sounder was provided by Keysight Technologies

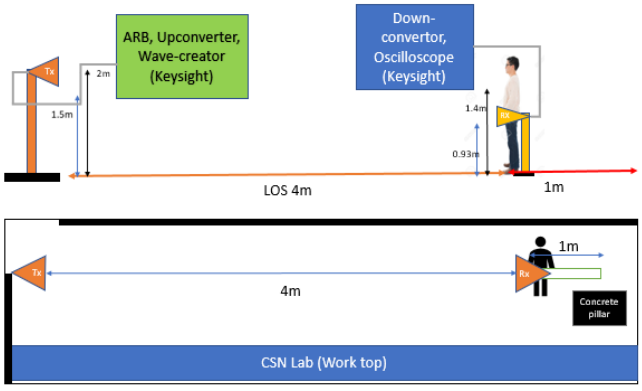

Fig. 3: Measurements setup performed in CSN Lab.

B. Measurements on a Walking Volunteer in the Laboratory Environment

The measurements depicted in Fig. 2 are performed in two steps. The first is to conduct reference measurements without a human body as shown in Fig. 3. A linear rail track controls the backward and forward for motion, producing negative and positive Doppler effect correspondingly. Meanwhile, both the P_{rx} and the CIR are recorded. Different antenna heights h_{tx} and h_{rx} are investigated and compared with the measurements performed in the Anechoic Chamber. In the second step, the same procedure is repeated but performed with a volunteer walking backwards and forward with the Rx antenna to investigate the attenuation. Fig. 5(a) and Fig. 5(b) show different P_{rx} observed and compared with the reference P_{rx}, measured at different h_{tx} and h_{rx} heights. The attenuation produced by the human body on the received signal in the shadow region can be obtained as

$$\text{attenuation (dB)} = P_{tx}(\text{dBm}) - P_{rx}(\text{dBm}) \quad (6)$$

Fig. 4: Measurement set up in the CSN Lab at UoB. A reference measurement is performed without a human body by using the linear rail track and compared to the results with a human body.

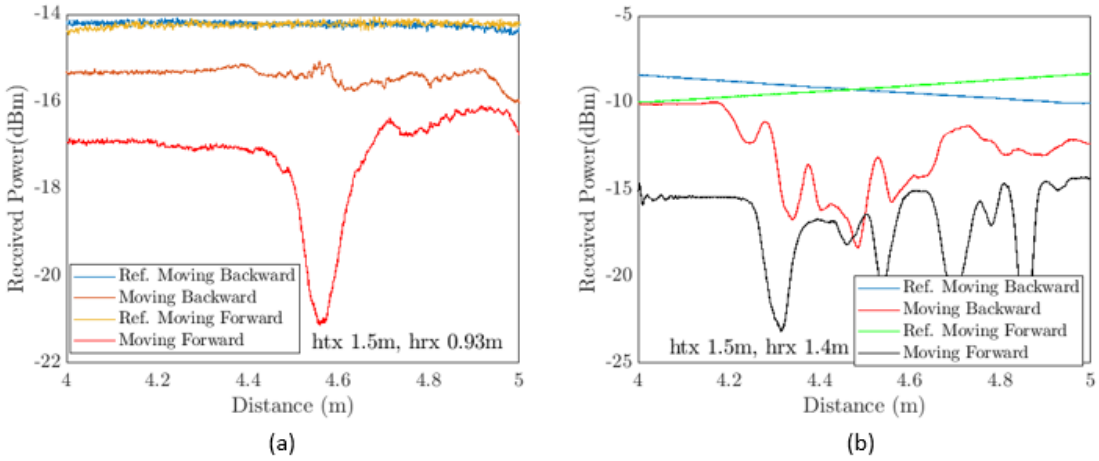

Fig. 5: P_{rx} in dBm against the distance. The notches in (a) and (b) are because the Rx antenna yaws during the move. The reference P_{rx} measurements in Fig.5(b) intersect at the middle position because the values the received power P_{rx} extracted from positive and negative Doppler shifts (due to moving forward and backward correspondingly) become identical at this position. However, reference measured P_{rx} is higher than the one with the human body because of the shadowing effect.

where P_{tx} is measured after the low noise amplifier (LNA) and it includes Tx antenna's gain and the attenuation of the RF cables. Similarly, P_{rx} includes Rx antenna's gain, the gain from LNA and attenuation produced by mm-wave frequency cables. Fig. 6 presents a complete comparison in a table for average P_{rx} with and without the human body as well as the average attenuation for measurements performed in the Anechoic chamber and the CSN Lab when there is a static human body and when there is a moving volunteer. It also compares the results with the reference measurements when the Rx is moving backwards and forwards which causes negative and positive Doppler shift respectively. Moreover, both the interference and the channel capacity are presented in the same table.

The RMS-DS is a measure of the channel dispersion in time which shows the time delay of strongest MPCs recorded by the channel sounder at the receiver's side [10]. Because of the rich scattering and reflections from the environment of the CSN lab, MPCs that take longer time until they are captured by the Rx antenna indicate a higher RMS-DS. Fig. 7(a) and Fig. 7(b) show the RMS-DS recorded during the measurements. The difference in RMS-DS for antenna heights are because of the presence of the volunteer and the yawing occurring during movement which adds fading to the received signal. For a mm-wave joint access point discussed in [11], the dispersion time of the channel can be controlled by steering the beamwidth, the antennas positions, and the antennas heights. Further, when MPCs travel shorter distances to reach Rx antenna, the resultant P_{rx} will be high, and any attenuation of the mm-wave signal in the shadow region produced because of the human body will be less. This research takes into account that the volunteer is (i) initially static, (ii) then walks backward during the first measurement's run which continues for 17.7s, (iii) walks forward during the final measurement's run, and (iv) becoming static by the end of the measurement's run. In all the cases, shadow regions are created.as indicated in [7]. Further, a lower measured P_{rx} caused by the antenna's de-pointing occurs, because the Rx antenna yaws whilst the volunteer walks backwards and forward. Since the beams from the Tx antenna points in the direction

Anechoic Chamber static Human body	Scenario	Average Pr dBm	Average Pr with/Without Human body in dBm	Attenuation with human body in dB	CSN Lab Static Human body	Average attenuation in dB before moving backwards	Average Attenuation in dB after moving forwards	CSN Lab Moving Human body Backwards Effect	Average ref. Pr dBm	Average Pr dBm	Average Pr diff. dBm	Ref. Attenuation in dB	Attenuation in dB	Shadowing w/m Fig. 1a	Average Channel Capacity Gbits/sec	CSN Lab Moving Human body Forwards Effect	Average ref. Pr dBm	Average Pr dBm	Average Pr diff. dBm	Ref. Attenuation in dB	Attenuation dB	Shadowing w/m Fig. 1b	Average Channel Capacity Gbits/sec
	hTx = 2m, hRx = 0.93 m	-23.97	0.08	48.72		51	51.29		-21.69	-28.13	0.71	46.69	49.71	-18.3	17.6		-21.82	-24.36	-3	46.82	49.36	-23.96	15.7
	hTx = 1.5m, hRx = 0.93 m	-17.25	2.89	41.96		40.35	41.99		-14.23	-15.4	-4.37	39.48	41.04	-8.09	14.9		-14.23	-16.93	-2.84	39.48	42.65	-11.19	14
	hTx = 1.5m, hRx = 1.4 m	-12.2	2.21	37.08		35.09	39.34		-9.26	-12.86	-1.94	35.05	37.86	-187	12.6		-9.18	-16.89	2.18	34.18	38.8	-254.8	12.6

Fig. 6: Comparison between different measurements performed in the Anechoic chamber and the CSN Lab at different Tx and Rx antenna heights h_{tx} and h_{rx} correspondingly in the presence of a volunteer.

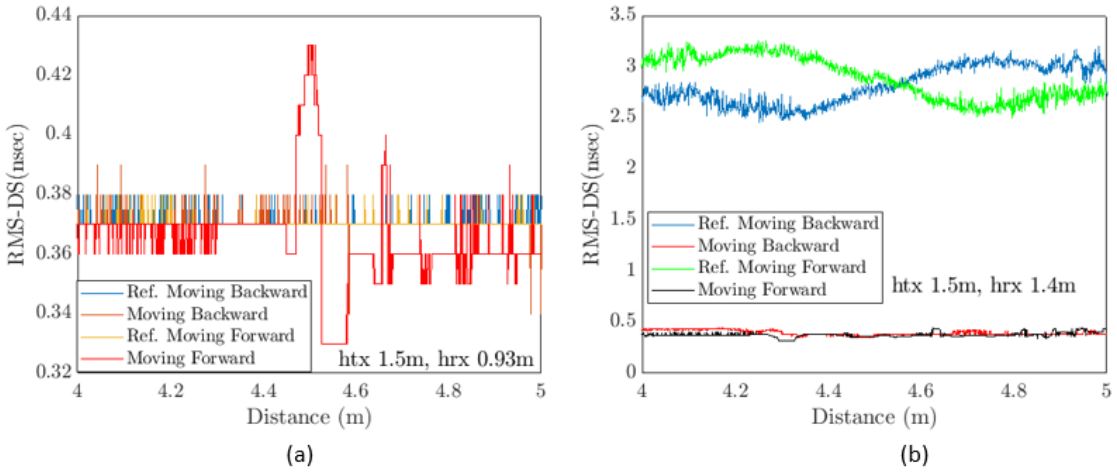

Fig. 7: RMS-DS relative to the distance in metres. The highest RMS-DS is observed when h_{tx} and h_{rx} are 1.5m and 1.4m correspondingly because of the yawing occurring whilst Rx antenna moves with the human body backwards and forward which causes antenna de-pointing. Consequently, the channel experiences high time and frequency dispersion. In Fig. 7 (b), the reference RMS-DS measurements performed in the CSN Lab intersect. This is because at this position, the Lab environment which causes the MPCs and hence the recorded RMS-DS become identical.

of the boresight of Rx antenna, different h_{tx} and h_{rx} heights are investigated. The yaw occurring in conjunction with the absorption of the radiated power by the human body reduces the level of P_{rx} [2]. However, by having multiple access points for a mm-wave system with different HPBWs as discussed in [11], MBA will improve, reducing the attenuation of the received mm-wave signal in the shadow region.

V. Conclusion

The shadow region of the human body is modelled, the shadow coefficient is derived and mm-wave signal attenuation produced in the shadow region of the human body during movement is investigated in this paper. The attenuation in the shadow region of the human body improves if h_{tx} and h_{rx} are adjusted appropriately or multiple access antennas are employed. The differences in attenuation between the reference measurements and real measurements with the volunteer computed from the P_{rx} at different h_{tx} and h_{rx} are less than 4dB. Since the investigation is focusing on a mobile device at mm-wave 5G, the attenuation in the shadow region is also is investigated when there is movement which produces either negative or positive Doppler effects. Further, an appropriate control on the antennas heights and beamwidth results in lower shadow and less dispersion time in the channel although there is a human body in the shadow region. Hence strong MPCs will be received with a short RMS-DS and this mitigates the attenuation. Finally, the relation developed between the shadow and the channel capacity decides which h_{tx} and h_{rx} can be considered for signal attenuation in the shadow region of the human body.

References

[1] S. Singh, M. N. Kulkarni, A. Ghosh, and J. G. Andrews, "Tractable model for rate in self-backhauled millimeter wave cellular networks," *IEEE Journal on Selected Areas in Communications*, vol. 33, no. 10, pp. 2196–2211, 2015.

[2] M. Zhadobov, N. Chahat, R. Sauleau, C. Le Quement, and Y. Le Drean, "Millimeter-wave interactions with the human body: state of knowledge and recent advances," *International Journal of Microwave and Wireless Technologies*, vol. 3, no. 2, pp. 237–247, 2011.

[3] V. Raghavan, L. Akhoondzadeh-Asl, V. Podshivalov, J. Hulten, M. A. Tassoudji, O. H. Koymen, A. Sampath, and J. Li, "Statistical blockage modeling and robustness of beamforming in millimeter-wave systems," *IEEE Transactions on Microwave Theory and Techniques*, vol. 67, no. 7, pp. 3010–3024, 2019.

[4] W. Hong, K. Baek, and S. Ko, "Millimeter-wave 5g antennas for smartphones: Overview and experimental demonstration," *IEEE Transactions on Antennas and Propagation*, vol. 65, no. 12, pp. 6250–6261, 2017.

[5] M. Heino, C. Icheln, and K. Haneda, "Self-user shadowing effects of millimeter-wave mobile phone antennas in a browsing mode," in *2019 13th European Conference on Antennas and Propagation (EuCAP)*, 2019, pp. 1–5.

[6] G. R. MacCartney, T. S. Rappaport, and S. Rangan, "Rapid fading due to human blockage in pedestrian crowds at 5g millimeter-wave frequencies," in *GLOBECOM 2017-2017 IEEE Global Communications Conference*. IEEE, 2017, pp. 1–7.

[7] Q. Wang, X. Zhao, S. Li, M. Wang, S. Sun, and W. Hong, "Attenuation by a human body and trees as well as material penetration loss in 26 and 39 ghz millimeter wave bands," *International Journal of Antennas and Propagation*, vol. 2017, 2017.

[8] T. Yokouchi, K. Akimoto, M. Motoyoshi, S. Kameda, and N. Suematsu, "Evaluation of channel capacity of millimeter-wave wban considering human body blocking in user-dense condition," in *2019 Eleventh International Conference on Ubiquitous and Future Networks (ICUFN)*, 2019, pp. 57–59.

[9] K. A. Al Mallak, M. Beach, T. H. Loh, and G. Hilton, "Characterisation of doppler shift in millimetre wave vehicular channel," IET APC2019.

[10] X. Zhao, Q. Wang, S. Li, M. Wang, and S. Sun, "Wideband millimeter-wave channel characterization in an open office at 26 ghz," *Wireless Personal Communications*, vol. 97, no. 4, pp. 5059–5075, 2017.

[11] M. N. Soorki, M. J. Abdel-Rahman, A. MacKenzie, and W. Saad, "Joint access point deployment and assignment in mmwave networks with stochastic user orientation," in *2017 15th International Symposium on Modeling and Optimization in Mobile, Ad Hoc, and Wireless Networks (WiOpt)*. IEEE, 2017, pp. 1–6.